HHS Public Access

Author manuscript

J Neurointerv Surg. Author manuscript; available in PMC 2016 December 01.

Published in final edited form as:

J Neurointerv Surg. 2015 December ; 7(12): 931–935. doi:10.1136/neurintsurg-2014-011412.

Hemodynamic Analysis of Fast and Slow Aneurysm Occlusions by Flow Diversion in Rabbits

BongJae Chung[1], **Fernando Mut**[1], **Ramanathan Karidvel**[2], **Ravi Lingineni**[4], **David F. Kallmes**[2,3], and **Juan R. Cebral**[1]

[1]Center for Computational Fluid Dynamics, College of Sciences, George Mason University, Fairfax, Virginia, USA

[2]Department of Radiology, Mayo Clinic, Rochester, Minnesota, USA

[3]Department of Neurosurgery, Mayo Clinic, Rochester, Minnesota, USA

[4]Department of Health Sciences and Research, Mayo Clinic, Rochester, Minnesota, USA

Abstract

Purpose—To assess hemodynamic differences between aneurysms that occlude rapidly versus those occluding in delayed fashion after flow diversion in rabbits.

Methods—Thirty six elastase induced aneurysms in rabbits were treated with flow diverting devices. Aneurysm occlusion was assessed angiographically immediately prior to sacrifice at one (n=6), two (n=4), four (n=8) or eight (n=18) weeks after treatment. Aneurysms were classified into a fast occlusion group if they were completely or near completely occluded at 4 weeks or earlier, and into a slow occlusion group if they remained incompletely occluded at 8 weeks. The immediate post-treatment flow conditions in aneurysms of each group were quantified using subject-specific computational fluid dynamics and statistically compared.

Results—Nine aneurysms were classified into the fast occlusion group and six into the slow occlusion group. Aneurysms in the fast occlusion group were on average significantly smaller (fast=0.9 cm, slow=1.393 cm, p=0.024), and had smaller ostia (fast=0.144 cm^2, slow=0.365 cm^2, p=0.015) than aneurysms in the slow occlusion group. They also had lower mean post-treatment inflow rate (fast=0.047 mL/s, slow=0.155 mL/s, p=0.0239), kinetic energy (fast=0.519 erg, slow=1.283 erg, p=0.0468), and velocity (fast=0.221 cm/s, slow=0.506 cm/s, p=0.0582). However, the differences of the latter two variables were only marginally significant.

Corresponding Author: BongJae Chung, PhD, Center for Computational Fluid Dynamics, College of Sciences, George Mason University, 4400 University Drive, MSN 6A2, Fairfax, VA 22030, USA, Phone: 703-993-4078, bchung5@gmu.edu.

COMPETING INTERESTS

None

CONTRIBUTORS

BC and FM: performed CFD simulations, edited the manuscript; RK: performed animal experiments, collected data, edited the manuscript; RL: performed statistical analysis; DK and JC: conceived the work, analyzed and interpreted the results, drafted the manuscript.

DATA SHARING STATEMENT

Computational models are freely available upon request.

Conclusions—Hemodynamic conditions after flow diversion treatment of cerebral aneurysms in rabbits are associated to the subsequent aneurysm occlusion time. Specifically, smaller inflow rate, kinetic energy, and velocity seem to promote faster occlusions, especially in smaller and small-necked aneurysms. These results are consistent with previous studies based on clinical series.

Keywords

cerebral aneurysm; flow diversion; hemodynamics; rabbit model; occlusion time

INTRODUCTION

Flow diversion is increasingly being used to treat wide necked intracranial aneurysms that are difficult to treat with coils alone[1–3]. However, flow diversion does not immediately exclude the aneurysm from the circulation. Therefore until the aneurysm thromboses and occludes it remains exposed to mechanical loads and biological processes that could potentially cause its rupture[4]. Presumably reducing the time it takes to completely occlude an aneurysm could prevent complications such as delayed ruptures[45]. Predicting or controlling the occlusion time after flow diversion is therefore important to improve the outcomes of these procedures and avoid complications. The purpose of this study was to assess the differences in the hemodynamic environment generated immediately after placement of flow diverting devices between aneurysms that occluded quickly and aneurysms that remained patent in a series of experimentally created aneurysms in rabbits.

METHODS

Animal Models

A total of 36 elastase-induced aneurysms were created in New Zealand white rabbits, following the approach described by Altes et al.[6]. Four weeks after their creation the aneurysms were imaged with 3D rotational angiography (3DRA) and flow velocities in the surrounding vessels were measured with Doppler Ultrasound (DUS). Subsequently, the aneurysms were treated with a FD device (Pipeline Embolization Device, Covidien). Two days before embolization, the subjects were premedicated with aspirin (10 mg/Kg PO) and clopidogrel (10 mg/kg PO). This medication regime was continued for one month after embolization. Some of the rabbits employed in this work were used as part of other studies[78] entirely unrelated to the current study. This animal research was conducted with appropriate institutional approvals.

Angiographic Evaluation

The animals were sacrificed within one week (n=6), at 2 weeks (n=4), at 4 weeks (n=8), and at 8 weeks (n=18) after treatment. Immediately prior to sacrifice angiographic imaging including 3DRA was repeated and the degree of aneurysm occlusion was categorized as: a) complete occlusion – no remnant, b) near complete occlusion – small remnant, c) incomplete occlusion – substantial filling of the aneurysm.

Hemodynamics Modeling

Computational fluid dynamics (CFD) models of the aneurysms were constructed using subject-specific vascular geometries derived from the pre-treatment 3DRA images and pulsatile flow conditions from the DUS measurements[7]. Models of the implanted FD devices were created and virtually deployed into the vascular models[9]. Vessel walls were assumed rigid, blood density was set to ρ=1.0 g/cm^3 and the Newtonian blood viscosity to μ=0.04 Poise. The unsteady incompressible Navier-Stokes equations were numerically solved using finite elements and adaptive immersed unstructured grids[10].

Data Analysis

Aneurysms were classified into two groups according to the end-time (time to sacrifice after treatment) and the degree of occlusion. Group 1, or “fast occlusion” group, included aneurysms that were completely or near completely occluded within one week, at 2 weeks or at 4 weeks. Group 2, or “slow occlusion” group, included aneurysms that were incompletely occluded at 8 weeks. In order to keep the fast and slow occlusion groups well defined and with no overlap, subjects not within these two groups were excluded from further analysis. The geometry and post-treatment hemodynamics of each aneurysm were characterized by computing a number of variables from the 3D CFD models. All variables considered were averaged over the aneurysm region and over the cardiac cycle. Exact definitions of the variables can be found in previous reports[81112]. The geometric and hemodynamic variables computed over the slow and fast occlusion groups were then statistically compared using the non-parametric Wilcoxon rank-sum test. Differences were consider significant if the p-values were smaller than 0.05 (95% confidence). All statistical analyses were performed using the SAS System (version 9.4, Cary, NC).

RESULTS

The end time, degree of occlusion and corresponding occlusion group of each aneurysm are presented in Table 1. A total of 6 aneurysms were classified into the slow occlusion group and 9 into the fast occlusion group. The mean and standard deviation of geometric and hemodynamic variables computed over these two groups are presented in Table 2 along with the corresponding p-values.

Ratios of mean geometric and hemodynamic variables of the slow over the fast occlusion groups are graphically presented in Figure 1. Bars above 1 indicate that the mean value of the slow occlusion group is larger than the mean value of the fast occlusion group. Statistically significant differences are indicated by a * above the corresponding bar.

Aneurysms in the fast occlusion group had significantly lower mean size (fast=0.900 cm, slow=1.393 cm, p=0.024), volume (fast=0.205 cm^3, slow=0.723 cm^3, p=0.030), area (fast=0.982 cm^2, slow=1.806 cm^2, p=0.038), and neck area (fast=0.144 cm, slow=0.365 cm^2, p=0.015), than aneurysms in the slow occlusion group. They also had lower mean post-treatment inflow rate (fast=0.047 mL/s, slow=0.155 mL/s, p=0.0239), kinetic energy (fast=0.519 erg, slow=1.283 erg, p=0.0468), and velocity (fast=0.221 cm/s, slow=0.506 cm/s, p=0.0582). However, the differences of the latter two variables were only marginally

significant. The inflow concentration, shear rate, vorticity, viscous dissipation and wall shear stress tended to be larger in the slow occlusion group but there was no statistical significance ($p>0.05$). The maximum and minimum WSS, OSI, the area under low WSS, the flow complexity (corelen) and stability (podent), and mean aneurysm transit time, as well as the aspect ratio and aneurysm depth were not statistically different between the two groups ($p>0.05$).

Flow visualizations of three example aneurysms are presented in Figure 2. From top to bottom this figure shows: iso-velocity (v=10 cm/s) before and after treatment and velocity streamlines before and after treatment. The first aneurysm (left column) was completely occluded before 1 week (fast occlusion), the second aneurysm (center column) was completely occluded at 4 weeks (fast occlusion), and the third aneurysm was incompletely occluded at 8 weeks (slow occlusion). It can be seen that immediately after treatment the inflow stream into aneurysms 1 and 2 are substantially reduced while in aneurysm 3 there is still a notable inflow into the aneurysm. The flow pattern in aneurysm 1 changed significantly after treatment. In particular, the inflow shifted to the proximal end of the neck and the intra-saccular streamlines followed a simpler and smoother trajectory. Aneurysm 2 follows the same general trend but with a slightly larger flow activity within the aneurysm sac. The flow structure in aneurysm 3 did not change markedly, although the blood speed along the streamlines was reduced.

DISCUSSION

Currently, there is no reliable technique to evaluate flow diversion treatments of intracranial aneurysms and to predict their long term outcomes. Previous studies have focused on the identification of qualitative and/or quantitative characteristics that could be used to prognosticate the outcomes of FD therapies[13–18]. However, the effects of flow diverting devices and the underlying mechanisms governing the thrombosis and occlusion of cerebral aneurysms are still not well understood.

Our current study used rabbit models to demonstrate that the flow conditions created immediately after placement of FD devices are quantitatively different between aneurysms that subsequently occluded quickly compared to aneurysms that remained patent for a longer period of time. In particular, the flow diverters more efficiently blocked the inflow stream and the resulting mean aneurysm velocity and flow activity were significantly smaller in fast occluding aneurysms. In the present study no balloons were used to expand the devices, and all devices were reasonably well appositioned against the parent artery wall covering the entire aneurysm orifice, except for two aneurysms of the slow occlusion group. In these two cases, the proximal end of the devices were not completely opposed to the wall which allowed a thin flow stream to slide between the device and the wall and enter the aneurysm (see aneurysm 3 in Figure 2). Imperfect deployments can have a substantial impact on the occlusion time and outcome of FD procedures.

Our results are consistent with previous studies based on clinical series[19,20]. This not only adds support to the validity of the rabbit aneurysm models but also confirms the idea that post-treatment flow conditions could potentially be used to assess the technical success of

FD procedures and to predict the occlusion times and long term outcomes. In particular, our study indicates that the mean aneurysm velocity which can potentially be measured with dynamic angiography[20] is a good predictor of occlusion time after FD treatment. However, in clinical situations there may be other factors besides hemodynamics and morphology that could affect the occlusion time after FD, including response to anti-platelet medication, co-morbidities like diabetes known to alter vascular response to implants, habits like smoking that alter platelet function and tissue repair, etc.

This study suffers from a number of limitations associated to assumptions and approximations made in the CFD modeling such as rigid walls, Newtonian rheology, idealized inflow profiles, etc. as well as limitations of the rabbit models such as flow reversal in the parent artery which does not occur in human cerebral arteries, and limited serial imaging that prevents visualization of the progression of aneurysmal occlusion. Nevertheless, these models allowed us to quantitatively compare the subject-specific hemodynamics between fast and slow aneurysm occlusion groups, and to identify target flow characteristics that could be used to accelerate the healing process after flow diversion and ultimately improve outcomes. These findings need to be further investigated and confirmed with larger series.

CONCLUSIONS

Hemodynamic conditions experimentally created immediately after flow diversion treatment of cerebral aneurysms in rabbits are associated to the subsequent aneurysm occlusion time. Specifically, smaller inflow rate, kinetic energy, and intra-saccular velocity seem to promote faster occlusions. These results are consistent with previous studies based on clinical series, and could be used to prognosticate the long term outcomes of flow diversion therapies.

Acknowledgments

We thank Covidien Inc. for generously providing flow diverters.

FUNDING

This work was supported by the National Institutes of Health (grant# NS076491).

References

1. Saatci I, Yavuz K, Ozer C, Geyik S, Cekirge HS. Treatment of Intracranial Aneurysms Using the Pipeline Flow-Diverter Embolization Device: A Single-Center Experience with Long-Term Follow-Up Results. AJNR American journal of neuroradiology. 2012; 33(8):1436–46. [PubMed: 22821921]
2. Lylyk P, Miranda C, Ceratto R, Ferrario A, Scrivano E, Luna H, et al. Curative endovascular reconstruction of cerebral aneurysms with the pipeline embolization device: the Buenos Aires experience. Neurosurgery. 2009; 64(4):632–42. [PubMed: 19349825]
3. Nelson PK, Lylyk P, Szikora I, Wetzel SG, Wanke I, Fiorella D. The pipeline embolization device for the intracranial treatment of aneurysms trial. AJNR American journal of neuroradiology. 2011; 32(1):34–40. [PubMed: 21148256]
4. Kulcsar Z, Houdart E, Bonafe A, GP, Millar J, Goddard AJ, et al. Intra-aneurysmal thrombosis as a possible cause of delayed aneurysm rupture after flow-diversion treatment. AJNR American journal of neuroradiology. 2011; 32(1):20–25. [PubMed: 21071538]

5. Cebral JR, Mut F, Raschi M, Scrivano E, Ceratto R, Lylyk P, et al. Aneurysm Rupture Following Treatment with Flow-Diverting Stents: Computational Hemodynamics Analysis of Treatment. AJNR American journal of neuroradiology. 2011; 32(1):27–33. [PubMed: 21071533]
6. Altes TA, Cloft HJ, Short JG, DeGast A, Do HM, Helm GA, et al. 1999 ARRS Executive Council Award. Creation of saccular aneurysms in the rabbit: a model suitable for testing endovascular devices. American Roentgen Ray Society. American Journal of Roentgenology. 2000; 174(2):349–54. [PubMed: 10658703]
7. Cebral JR, Mut F, Raschi M, Ding YH, Kadirvel R, Kallmes DF. Strategy for analysis of flow diverting devices based on multi-modality image-based modeling. Int J Num Meth Biomed Eng. 2014; in press. doi: 10.1002/cnm.2638
8. Cebral JR, Mut F, Raschi M, Hodis S, Ding YH, Erickson BJ, et al. Analysis of Hemodynamics and Aneurysm Occlusion after Flow-Diverting Treatment in Rabbit Models. AJNR. American journal of neuroradiology. 2014; in press. doi: 10.3174/ajnr.A3913
9. Mut F, Cebral JR. Effects of Flow-Diverting Device Oversizing on Hemodynamics Alteration in Cerebral Aneurysms. AJNR American journal of neuroradiology. 2012; 33(10):2010–16. [PubMed: 22555581]
10. Appanaboyina S, Mut F, Löhner R, Putman CM, Cebral JR. Simulation of intracranial aneurysm stenting: techniques and challenges. Computer Methods in Applied Mechanics and Engineering. 2009; 198(45–46):3567–82.
11. Mut F, Löhner R, Chien A, Tateshima S, Viñuela F, Putman CM, et al. Computational hemodynamics framework for the analysis of cerebral aneurysms. Int J Num Meth Biomed Eng. 2011; 27(6):822–39.
12. Byrne G, Mut F, Cebral JR. Quantifying the large-scale gemodynamics of intracanial aneurysms. AJNR American journal of neuroradiology. 2014; 35(2):333–38. [PubMed: 23928142]
13. Lieber BB, Stancampiano AP, Wakhloo AK. Alteration of hemodynamics in aneurysm models by stenting: influence of stent porosity. Annals of Biomedical Engineering. 1997; 25(3):460–69. [PubMed: 9146801]
14. Lieber BB, Livescu V, Hopkins LN, Wakhloo AK. Particle image velocimetry assessment of stent design influence on intra-aneurysmal flow. Annals of Biomedical Engineering. 2002; 30:768–77. [PubMed: 12220077]
15. Seong J, Wakhloo AK, Lieber BB. In Vitro Evaluation of Flow Divertors in an Elastase-Induced Saccular Aneurysm Model in Rabbit. Journal of Biomechanical Engineering. 2007; 129(6):863–72. [PubMed: 18067390]
16. Sadasivan C, Cesar L, Seong J, Wakhloo AK, Lieber BB. Treatment of rabbit elastase-induced aneurysm models by flow diverters: development of quantifiable indexes of device performance using digital subtraction angiography. IEEE Trans Med Imaging. 2009; 28(7):1117–25. [PubMed: 19164085]
17. Sadasivan C, Lieber BB, Gounis MJ, Lopes DK, Hopkins LN. Angiographic quantification of contrast medium washout from cerebral aneurysms after stent placement. AJNR American Journal of Neuroradiology. 2002; 23:1214–21. [PubMed: 12169482]
18. Pereira VM, Bonnefous O, Ouared R, Brina O, Stawiaski J, Aerts H, et al. A DSA-Based Method Using Contrast-Motion Estimation for the Assessment of the Intra-Aneurysmal Flow Changes Induced by Flow-Diverter Stents. AJNR American journal of neuroradiology. 2013; 34(3):805–15.
19. Mut F, Raschi M, Scrivano E, Bleise C, Chudyk J, Ceratto R, et al. Association between hemodynamic conditions and occlusion times after flow diversion in cerebral aneurysms. Journal of neurointerventional surgery. 2014; in press. doi: 10.1136/neurintsurg-2013-011080
20. Kulcsar Z, Augsburger L, Reymond P, Pereira VM, Hirsch S, Mallik AS, et al. Flow diversion treatment: intra-aneurismal blood flow velocity and WSS reduction are parameters to predict aneurysm thrombosis. Acta Neurochir (Wien). 2012; 154(10):1827–34. [PubMed: 22926629]

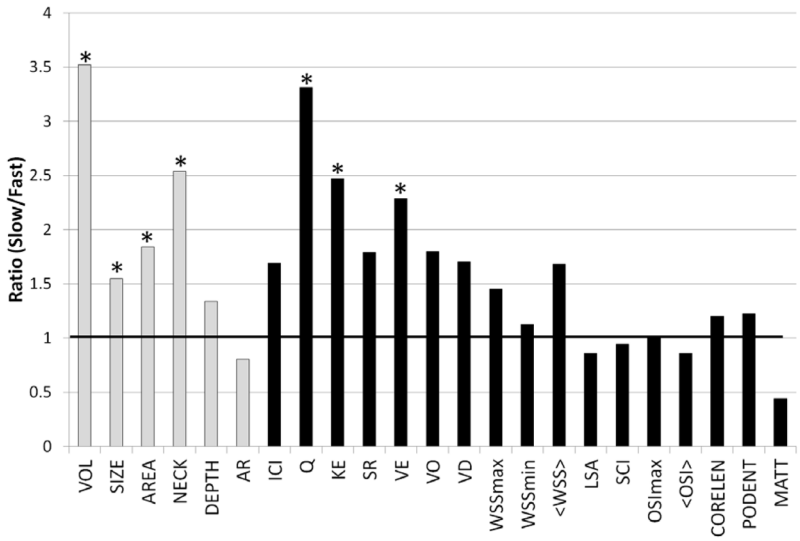

Figure 1.

Ratio of average geometric (gray bars) and hemodynamic (black bars) variables of the slow over the fast occlusion groups. Statistically significant differences between the two groups are marked with a *.

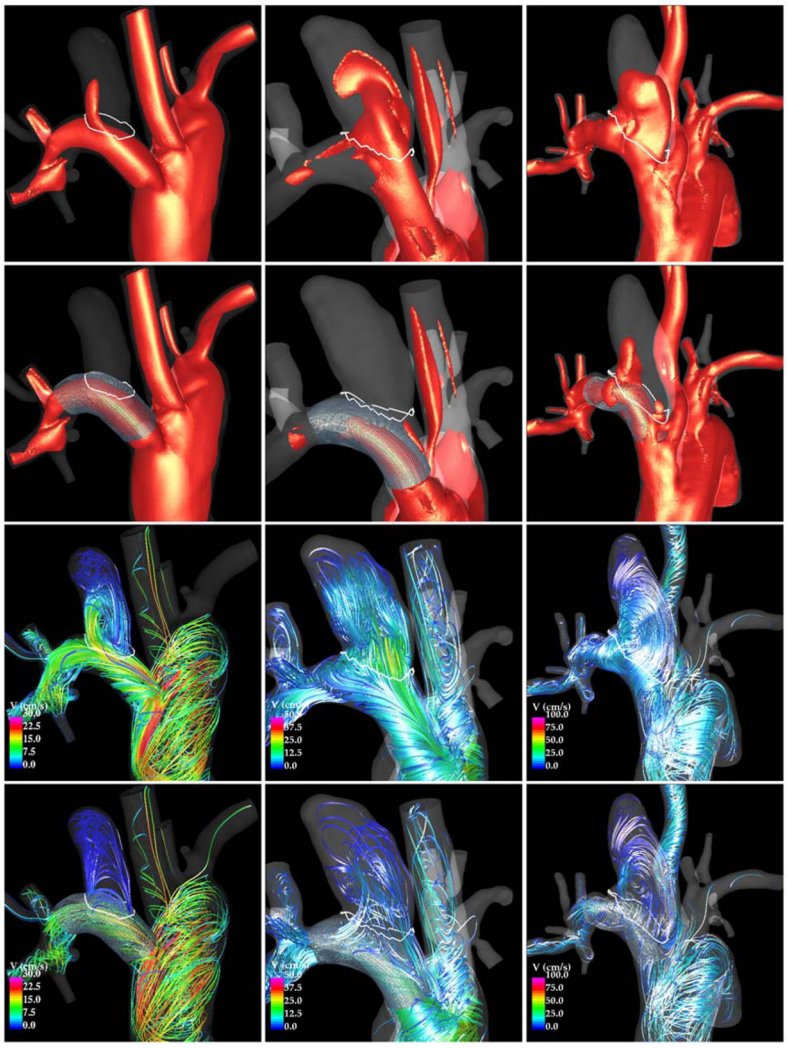

Figure 2.

Flow visualizations in aneurysms occluded at 1 week (left column) and 4 weeks (center column), and in an aneurysm incompletely occluded at 8 weeks (right column). Each column shows, from top to bottom: iso-velocity pre-treatment, iso-velocity post-treatment, flow streamlines pre-treatment, and flow streamlines post-treatment.

Table 1

End point, occlusion status and grouping of aneurysms.

Case	End-time	Occlusion	Group
1	< 1 week	incomplete	-
2	< 1 week	incomplete	-
3	< 1 week	incomplete	-
4	< 1 week	near complete	fast
5	< 1 week	near complete	fast
6	< 1 week	complete	fast
7	2 weeks	incomplete	-
8	2 weeks	near complete	fast
9	2 weeks	incomplete	-
10	2 weeks	incomplete	-
11	4 weeks	near complete	fast
12	4 weeks	near complete	fast
13	4 weeks	incomplete	-
14	4 weeks	complete	fast
15	4 weeks	incomplete	-
16	4 weeks	incomplete	-
17	4 weeks	near complete	fast
18	4 weeks	near complete	fast
19	8 weeks	incomplete	slow
20	8 weeks	incomplete	slow
21	8 weeks	incomplete	slow
22	8 weeks	incomplete	slow
23	8 weeks	incomplete	slow
24	8 weeks	incomplete	slow
25	8 weeks	near complete	-
26	8 weeks	near complete	-
27	8 weeks	near complete	-
28	8 weeks	near complete	-
29	8 weeks	near complete	-
30	8 weeks	complete	-
31	8 weeks	complete	-
32	8 weeks	complete	-
33	8 weeks	complete	-
34	8 weeks	complete	-
35	8 weeks	complete	-
36	8 weeks	complete	-

Table 2

Summary statistics of geometric and hemodynamic variables over the slow and fast occlusion groups.

Variable	Slow occlusion		Fast occlusion		P-value
	Mean	Stdev	Mean	Stdev	
VOL – aneurysm volume	0.723	0.495	0.205	0.238	0.0299
SIZE – maximum diameter	1.393	0.294	0.900	0.235	0.0239
AREA – aneurysm area	1.806	0.678	0.982	0.372	0.0375
NECK – neck area	0.365	0.082	0.144	0.078	0.0151
DEPTH – maximum distance to neck	0.920	0.255	0.687	0.197	0.0891
AR – aspect ratio	1.238	0.375	1.539	0.427	0.3917
ICI – inflow concentration index	0.013	0.035	0.007	0.010	0.2817
Q – aneurysm inflow rate	0.155	0.095	0.047	0.053	0.0239
KE – kinetic energy	1.283	1.010	0.519	0.967	0.0468
SR – shear rate	7.160	3.326	4.009	3.514	0.0722
VE - velocity	0.506	0.298	0.221	0.241	0.0582
VO - vorticity	7.714	4.220	4.294	4.221	0.0891
VD – viscous dissipation	2.807	1.664	1.650	2.353	0.1968
WSSmax – maximum WSS	92.635	95.690	63.854	32.524	0.7726
WSSmin – minimum WSS	0.000	0.000	0.000	0.000	0.6862
<WSS> - mean WSS	0.684	0.233	0.407	0.275	0.0891
LSA – low WSS area	59.908	28.391	69.925	29.239	0.5274
SCI – WSS concentration index	10.888	15.718	11.549	9.296	0.3917
OSImax – maximum oscillatory shear index	0.489	0.008	0.484	0.031	0.6042
<OSI> - mean oscillatory shear index	0.319	0.119	0.371	0.109	0.2817
CORELEN – vortex coreline length	1.352	0.562	1.127	0.469	0.6862
PODENT – entropy of POD modes	0.720	0.250	0.588	0.206	0.3335
MATT – mean aneurysm transit time	6.222	4.441	14.060	15.209	0.5274

J Neurointerv Surg. Author manuscript; available in PMC 2016 December 01.